CHAPTER 133

Suspended Sediment Transport in Inner Shelf Waters During Extreme Storms

O.S. Madsen[1] T.A. Chisholm[2] and L.D. Wright[2]

Abstract

The paper presents a simple model for the prediction of longshore and crosshore suspended sediment transport rates outside the surf zone in water depths less than 20 m or so. The model consists of a depth-resolving hydrodynamic component, which considers wind-induced currents in the presence of waves and includes the Coriolis effect. The hydrodynamic model component is coupled with a model for the mean suspended sediment concentration to produce a prediction of the depth-varying mean suspended sediment flux vector. In addition to specification of environmental conditions, *i.e.* waves and sediment characteristics as well as current driving forces (wind velocity and pressure gradient), the model requires three parameters: C_a, the wind-drag coefficient; k_N, the movable bed bottom roughness; and γ_0, the resuspension parameter. These three model parameters were determined (Madsen et al., 1993) from a subset of field data obtained in 13 m depth off Duck, North Carolina, during the severe "Halloween Storm" of 1991 and are used to perform a limited comparison between predicted and observed current velocity vectors and mean suspended sediment concentrations. The agreement is very encouraging and model prediction of an offshore loss of 22 m^3 sediment per m beach compares favorably with the loss of 27 to 54 m^3 obtained from beach profile surveys.

---

[1] R.M. Parsons Laboratory, Massachusetts Institute of Technology, Cambridge, MA 02139 USA

[2] Virginia Institute of Marine Science, College of William and Mary, Gloucester Point, VA 23062 USA

Introduction

The importance of storms to coastal change has been documented extensively. Storm-driven processes are also known to dominate sediment transport on the inner shelf, *i.e.* outside the surf zone in water depths up to 20 m or so. However, very little quantitative information is available on near-bottom currents, bed shear stresses and sediment fluxes for the reliable prediction of sediment transport processes on the inner shelf which forms an important link between the extensively studied processes within the surf zone and deeper continental shelf waters.

Across the inner shelf currents are induced by wind and pressure gradients more so than by wave-associated radiation stresses. This paper present a depth-resolving model for the wind-induced and pressure gradient driven (tidal) current in inner shelf waters along fairly straight coastlines. The bottom boundary condition for the current is specified in terms of the apparent bottom roughness experienced by currents in the presence of waves and is calculated from the theory of Madsen (1994). Since the determination of the apparent bottom roughness requires the current to be specified, an iterative solution procedure is necessary to solve for the depth-varying current velocity vector. In addition to wave-current interaction in the bottom boundary layer the model includes Coriolis effects, since crosshore sediment transport is sensitive to even minor changes of the current velocity vector's direction.

The current shear velocities and eddy viscosities obtained from the hydrodynamic model are used to predict the profiles of mean suspended sediment concentration. For the suspended sediment concentration the effect of waves is again manifesting itself through the specification of a reference concentration at the bottom. Mean suspended sediment fluxes are obtained from the product of current velocity and mean concentration, and integration over depth produces the total mean suspended sediment transport rate in the alongshore and crosshore directions.

The unique data set obtained during the severe "Halloween Storm" of 1991 is used to perform a limited comparison between observations and predictions by the hydrodynamic and sediment transport model. Although a small subset of this available field data set was used (Madsen et al., 1993) to determine empirical values for important model parameters (wind-drag coefficient, movable bed roughness, and resuspension parameter) this comparison is quite encouraging, as is the model's prediction of a net loss of sediment per meter beach during the entire "Halloween Storm" which is within a factor of two from the loss determined by beach profile surveys.

The Depth-Resolving Hydrodynamic Model

Under the assumptions of slowly varying forcing in space and time the equations governing the depth-dependent current velocities, $u = u(z)$ and $v = v(z)$ of a constant density, ρ, fluid in the horizontal xy-plane may be written

$$\frac{Du}{Dt} \simeq 0 = -\frac{1}{\rho}\frac{\partial p}{\partial x} + fv + \frac{\partial}{\partial z}\left(\nu_t \frac{\partial u}{\partial z}\right) \tag{1}$$

$$\frac{Dv}{Dt} \simeq 0 = -\frac{1}{\rho}\frac{\partial p}{\partial y} - fu + \frac{\partial}{\partial z}\left(\nu_t \frac{\partial v}{\partial z}\right) \tag{2}$$

in which $f = 1.45 \cdot 10^{-4}$ sin (latitute) s^{-1} is the Coriolis Parameter, z is the vertical coordinate ($z = 0$ at the bottom), the pressure gradients, $\partial p/\partial x$ and $\partial p/\partial y$, are assumed independent of z corresponding to hydrostatic pressure distribution and ν_t is a turbulent eddy viscosity.

Introducing the geostrophic current defined by

$$f\{U_g, V_g\} = -\frac{1}{\rho}\left\{\frac{\partial p}{\partial y}, -\frac{\partial p}{\partial x}\right\} \tag{3}$$

multiplication of (2) by $i = \sqrt{-1}$ followed by addition of (1) leads to a single governing equation

$$\frac{\partial}{\partial z}\left(\nu_t \frac{\partial W}{\partial z}\right) - ifW = 0 \tag{4}$$

in the complex velocity

$$W = (u - U_g) + i(v - V_g) \tag{5}$$

The complete analogy of (4) to the equation governing oscillatory turbulent bottom boundary layer for simple periodic waves, *e.g.* Eq. (4) of Madsen (1994), is noted. Here the Coriolis Parameter, f, replaces the radian frequency, ω, and the imaginary part of the solution of (4) represents the y-component of the velocity whereas it, in the wave boundary layer case, is without physical significance.

In order to solve (4) it is first necessary to specify the turbulent eddy viscosity, ν_t. Here we follow the suggestion of Madsen (1977) as did Jenter and Madsen (1989) by adopting an eddy viscosity which increases linearly with distance from a sheared boundary and is scaled by this boundary's shear velocity, $u_* = \sqrt{\tau/\rho}$. In the present case wind stress, τ_s, acts on the free surface, $z = h$, and a bottom stress, τ_c, acts on the bottom $z = 0$. The resulting model for ν_t therefore becomes

$$\nu_t = \begin{cases} \kappa u_{*c} z & \text{for} \quad 0 < z < z_m \\ \kappa u_{*s}(h - z) & \text{for} \quad z_m < z < h \end{cases} \tag{6}$$

in which κ = von Karman's constant ($\kappa = 0.4$), and z_m is the distance above the bottom at which the transition from bottom to surface shear dominated turbulence is made. This level is chosen, as suggested by Madsen (1977), to be scaled by the relative magnitude of the two shear velocities, *i.e.*

$$z_m = \frac{u_{*c}}{u_{*s} + u_{*c}} h \tag{7}$$

With ν_t given by (6) and (7) the general solution of (4) is obtained (Jenter and Madsen, 1989) in terms of zeroth order Kelvin functions

$$\begin{aligned} W = W_b = & A_b(ber2\sqrt{\zeta_b} + ibei2\sqrt{\zeta_b}) + \\ & B_b(ker2\sqrt{\zeta_b} + ikei2\sqrt{\zeta_b}) \quad \text{for} \quad 0 < \zeta_b < \zeta_{bm} \end{aligned} \tag{8}$$

and

$$\begin{aligned} W = W_s = & A_s(ber2\sqrt{\zeta_s} + ibei2\sqrt{\zeta_s}) + \\ & B_s(ker2\sqrt{\zeta_s} + ikei2\sqrt{\zeta_s}) \quad \text{for} \quad 0 < \zeta_s < \zeta_{sm} \end{aligned} \tag{9}$$

in which A_b, B_b, A_s and B_s are arbitrary complex constants, and the nondimensional vertical coordinates are given by

$$\zeta_b = \frac{zf}{\kappa u_{*c}} \quad \text{and} \quad \zeta_s = \frac{(h - z)f}{\kappa u_{*s}} \tag{10}$$

and ζ_{bm} and ζ_{sm} are the matching coordinates given by (10) with $z = z_m$.

The arbitrary constants in (8) and (9) are determined by the boundary condition at the surface

$$\left(\kappa u_{*s}\sqrt{\zeta_s}\frac{dW_s}{d(2\sqrt{\zeta_s})}\right)_{\zeta_s \to 0} = -\frac{1}{\rho}\left(\tau_{sx} + i\tau_{sy}\right) \tag{11}$$

in which the wind shear stress at the free surface is given by

$$\tau_s e^{i\phi_a} = \rho_a C_a U_a^2 e^{i\phi_a} = \tau_{sx} + i\tau_{sy} \tag{12}$$

with ρ_a being the air density, U_a the wind speed, ϕ_a the wind direction measured from the x-axis and C_a is the wind-drag coefficient; and the turbulent no-slip condition at the bottom

$$W_b = -(U_g + iV_g) \quad \text{at} \quad \zeta_b = \zeta_{bo} = \frac{z_{oa} f}{k u_{*c}} \tag{13}$$

in which z_{oa} denotes the apparent bottom roughness, *i.e.* the bottom roughness experienced by the current in the presence of waves (Madsen, 1994).

The additional conditions are supplied by the requirement of continuity of velocity and shear stress at the matching level, *i.e.*

$$W_b(\zeta_b = \zeta_{bm}) = W_s(\zeta_s = \zeta_{sm}) \tag{14}$$

and

$$u_{*c}\sqrt{\zeta_{bm}} \frac{dW_b}{d(2\sqrt{\zeta_b})}\bigg|_{\zeta_b=\zeta_{bm}} = -u_{*s}\sqrt{\zeta_{sm}} \frac{dW_s}{d(2\sqrt{\zeta_s})}\bigg|_{\zeta_s=\zeta_{sm}} \tag{15}$$

in which the minus signs in (11) and (15) are the result of ζ_s being proportional to $(h - z)$ rather than z.

Formally the arbitrary constants may be obtained by sloving (11) through (15). Series expansions for the zeroth order Kelvin functions and their derivatives found in Abramowitz and Stegun (1972; Chapter 9) greatly facilitate this task. However, the vertical coordinate used in the lower (bottom) layer depends on the bottom shear stress, $u_{*c} = \sqrt{\tau_c/\rho}$, which is *a priori* an unknown. The same is true for the apparent bottom roughness which depends on wave-current interaction within the wave bottom boundary layer and hence needs a specification of the current characteristics before it can be determined (see Madsen, 1994). Finally, the pressure gradients need to be determined (or known) in order to solve the problem.

The Bottom Shear Velocity, u_{*c}

To overcome the problem of an initially unknown value of the bottom shear stress, we proceed in an iterative manner by assuming a value of u_{*c} to obtain the solution for W_b and subsequently evaluate the bottom shear stress from

$$\tau_c e^{i\phi_c} = \rho\kappa u_{*c}\sqrt{\zeta_{bo}}\frac{dW_b}{d(2\sqrt{\zeta_b})}\bigg|_{\zeta_b=\zeta_{bo}} \tag{16}$$

which, since $\tau_c = \rho u_{*c}^2$, yields a "new" value of u_{*c}. When convergence has been achieved the angle ϕ_c denotes the direction of the bottom shear stress and hence the direction of the near-bottom current velocity.

The Apparent Bottom Roughness, z_{oa}

The evaluation of the apparent bottom roughness depends on the wave characteristics, the physical (movable bed) bottom roughness, k_N, and the current specification. The details of a spectral wave-current interaction model are presented by Madsen (1994). Here it suffices to mention that the wave motion is specified by a representative periodic wave of near-bottom orbital velocity amplitude, u_{br}, radian frequency, ω_r, and direction of propagation ϕ_{wr} (Eqs. (22), (23) and (24) in Madsen, 1994). From this information, along with k_N and an assumed current specified by its shear stress τ_c and direction ϕ_c, the solution of the wave-current interaction problem is detailed by Madsen (1994) and leads to a solution for the apparent bottom roughness obtained from Eq. (11) of Madsen (1994)

$$z_{oa} = \left(\frac{k_N}{30\delta_{wc}}\right)^{u_{*c}/u_{*r}}\delta_{wc} \tag{17}$$

in which δ_{wc} and u_{*r} denote the wave bottom boundary layer thickness and the shear velocity based on the maximum combined wave-current bottom shear stress, respectively, and are defined by Eqs. (36) and (26) of Madsen (1994).

Specifying the no-slip condition for the current in terms of the apparent roughness z_{oa}, avoids the determination of the current velocity profile within the wave boundary layer. This information is, however, needed for the evaluation of suspended sediment flux immediately above the bottom. With general reference to Madsen (1994) for details, we merely state the proper form for the current velocity profile within the wave bottom boundary layer as

$$u + iv = \frac{u_{*c}}{u_{*r}}\frac{u_{*c}}{\kappa}\ell n\frac{30z}{k_N}e^{i\phi_c} \tag{18}$$

valid for $z < \delta_{wc}$ with ϕ_c obtained from (16).

The Pressure Gradients, $\partial p/\partial x$ and $\partial p/\partial y$

It is consistent with the assumption of slow spatial variability to assume an essentially straight coastline. We therefore choose a coordinate system with a shore-parallel x-axis. Furthermore, limiting the model's application to water depths less than 10 to 20 m, corresponding to distances from shore of the order of at most 1 km or so, suggests that any crosshore depth-averaged current should be negligible.

For wind-dominated storm events the uniformity in the shore-parallel x-direction justifies the neglect of an alongshore mean surface slope and results in a pressure gradient of $\partial p/\partial x \simeq 0$. If the longshore mean surface slope cannot safely be assumed negligible an approximate methodology for obtaining an estimate of $\partial p/\partial x$ to be used in conjunction with the steady depth-resolving model is presented by Chisholm (1993) and is outlined in Appendix A.

Imposing the negligible crosshore mean current on the general solution yields the condition

$$\int_0^h v dz \simeq \int_0^h \Im \{W + iV_g\} dz = 0 \tag{19}$$

from which the crosshore pressure gradient, $\partial p/\partial y$, may be determined with W given by (8) and (9). For the simplest model application (3) shows that $V_g = 0$ since $\partial p/\partial x \simeq 0$.

Solution Strategy

To apply the depth-resolving hydrodynamic model it is assumed that the representative periodic wave characteristics, u_{br}, ω_r and ϕ_{wr} as defined by Madsen (1994) are known. From the wave conditions and knowledge of the bottom sediment characteristics the physical (movable bed) bottom roughness, k_N, may be estimated from, *e.g.* Wiberg and Harris (1994) for rippled bed or Madsen et al. (1993) for flat movable bed. The surface wind shear stress, is obtained from (12) with C_a estimated from, *e.g.* Wu (1982) or Madsen et al. (1993).

Assuming the wind to have a substantial longshore component an initial estimate of the bottom shear stress is obtained by considering the alongshore flow to be approximately described by as a Couette flow, *i.e.* $\tau_c = \rho u_{*c}^2 \simeq \tau_s \cos \phi_a$. With this shore-parallel current bottom shear stress "known" the wave-current interaction model by Madsen (1994) may be used to obtain a first estimate of the apparent bottom roughness, z_{oa}, from (17).

The depth-resolving hydrodynamic model may now be formally solved. The "unknown" crosshore pressure gradient, $\partial p/\partial y$ (or U_g), is obtained from

(19) and the bottom shear stress vector and shear velocity are upgraded by use of (16). We may now re-evaluate the apparent bottom roughness from (17) and continue the iteration until convergence has been achieved.

The Mean Suspended Sediment Transport Model

The concentration of suspended sediment is described by the diffusion equation. Limiting the model's applicability to slowly varying conditions in space and time, *i.e.* disregarding variations over the timescale of the wave motion, the equation governing the mean suspended sediment concentation, $c(z)$, reads

$$\frac{Dc}{Dt} \simeq 0 = \frac{\partial}{\partial z}\left(\nu_s \frac{\partial c}{\partial z}\right) + \frac{\partial}{\partial z}(w_f c) \tag{20}$$

in which $w_f (> 0)$ denotes the fall velocity of the sediment and ν_s is the eddy diffusivity.

The eddy differsivity is taken equal to the eddy viscosity used in the depth-resolving hydrodynamic model, *i.e.* $\nu_s = \nu_t$ with ν_t given by (6). The hydrodynamic model, however, did not explicitly include the description of the current profile in the immediate vicinity of the bottom, *i.e.* within the wave bottom boundary layer of thickness δ_{wc}. Within the wave boundary layer the eddy viscosity and hence the eddy diffusivity is given by the wave-current interaction model (see Madsen, 1994) and we therefore have

$$\nu_s = \begin{cases} \kappa u_{*r} z & 0 < z < \delta_{wc} \\ \kappa u_{*c} z & \delta_{wc} < z < z_m \\ \kappa u_{*s}(h - z) & z_m < z < h \end{cases} \tag{21}$$

Integration of (20) leads to an expression for the vertical flux of suspended sediment which, by virtue of the steady state assumption, must be zero and the resulting equation becomes

$$\frac{dc}{dz} = -\frac{w_f}{\nu_s} c \tag{22}$$

To solve this equation with ν_s given by (21) one boundary condition is needed.

The Reference Concentration

We adopt the reference concentration, c_R, specified at a given elevation, $z = z_R$, within the wave boundary layer, *i.e.* $z_R < \delta_{wc}$, as our boundary condition. Following Smith and McLean (1977) we assume the functional form of the mean reference concentration to be

$$c_R = \gamma_0 c_b \left(|\overline{\tau_b'}|/\tau_{cr} - 1 \right) \quad \text{at} \quad z = z_R = 7d \tag{23}$$

in which c_b is the volume concentration of sediment in the bed, τ_b' is the skin friction bottom shear stress due to the combined wave-current flow, τ_{cr} is critical shear stress for initiation of motion (Madsen and Grant, 1976), and γ_0 is the resuspension parameter. The functional form of (23) is supported by the simple bedload formula for saltating grains derived by Madsen (1991). Regarding the transport that takes place withhin the saltation layer as bedload (and therefore not to be included in the suspended load transport) the level at which the reference concentration is specified is taken as the top of the saltation layer which is approximated as $z_R = 7d$, with d being the diameter of the bottom sediment.

The skinfriction shear stress, τ_b', in (23) includes the contribution from wave motion. In fact, it is to be expected that $|\tau_b'|$ is dominated by wave action with currents playing only a secondary role in the suspension of bottom sediments. Since the intended application of the present model is for stormy conditions, we shall assume wave-dominance and take

$$\tau_b' \simeq \tau_w' = \tau_{wm}' \cos(\omega_r t + \phi_{\tau r}') \tag{24}$$

where $\phi_{\tau r}'$ is a phase angle which, in the present context, is of no importance, and

$$\tau_{wm}' = \frac{1}{2} \rho f_w' u_{br}^2 \tag{25}$$

is the maximum skinfriction bottom shear stress of the representative periodic wave defined by Madsen (1994) evaluated for a bottom roughness equal to the mean diameter of the bottom sediment. Given the functional form of (23) it follows logically that the representative periodic wave defined by Madsen (1994), *i.e.* not the "significant wave", is the proper choice for the determination of the mean reference concentration in combined wave-current boundary layer flows.

Introduction of (24) in (23) therefore results in a relatively simple expression for the mean reference concentration for wave-dominated flows

$$c_R = \gamma_0 c_b \left(\frac{2}{\pi} \frac{\tau_{wm}'}{\tau_{cr}} - 1 \right) \quad \text{at} \quad z = z_R = 7d \tag{26}$$

with τ'_{wm} given by (25) which is readily evaluated using formulas given by Madsen (1994). It is important to emphasize at this point that the empirical value of the resuspension parameter, γ_0, is intimately tied to the level, z_R, at which it is specified and to the particular theoretical model used to extrapolate actual concentration measurements from their level, to the chosen reference level. Wikramanayake (1992), using the present reference level obtained values of $\gamma_0 = 2 \cdot 10^{-3}$ and $2 \cdot 10^{-4}$ for rippled beds and flat movable beds, respectively. These values may be used for preliminary considerations, but it should be recognized that a great deal of uncertainty is associated with the specification of γ_0.

The Mean Suspended Sediment Concentration

With the mean concentration governed by (22), the eddy diffusivity given by (21) and the reference concentration specified by (26) the solution for the mean suspended sediment concentration is readily obtained.

Within the wave boundary layer, $z_R < z < \delta_{wc}$ we obtain

$$c = c_R \left(\frac{z}{z_R}\right)^{-\frac{w_f}{\kappa u_{*r}}} \qquad (27)$$

In the bottom layer of the water column, $\delta_{wc} < z < z_m$, integration of (21) and matching the concentration with (26) at $z = \delta_{wc}$ gives

$$c = c_R \left(\frac{\delta_{wc}}{z_R}\right)^{-\frac{w_f}{\kappa u_{*r}}} \left(\frac{z}{\delta_{wc}}\right)^{-\frac{w_f}{\kappa u_{*c}}} \qquad (28)$$

In the surface layer of the water column, $z_m < z < h$, the mean concentration is given by

$$c = c_R \left(\frac{\delta_{wc}}{z_R}\right)^{-\frac{w_f}{\kappa u_{*r}}} \left(\frac{z_m}{\delta_{wc}}\right)^{-\frac{w_f}{\kappa u_{*c}}} \left(\frac{h - z_m}{h - z}\right)^{-\frac{w_f}{\kappa u_{*s}}} \qquad (29)$$

Mean Suspended Sediment Transport

The complex current velocity profile

$$u + iv = W + U_g + iV_g \qquad (30)$$

is obtained from (3), (8) and (9), with (8) replaced by (18) within the wave boundary layer, for the three depth-intervals for which the mean concentrations of suspended sediments are given by (27) through (29). The depth-integrated complex suspended sediment flux vector is evaluated from

$$q_{sx} + iq_{sy} = \int_{z_R}^{h} (u + iv) c dz \tag{31}$$

Extension of Model to Sediment Mixtures

The preceeding presentation of the mean suspended sediment transport model treated the sediment as uniform, *i.e.* represented by a single size-class of diameter d. The model is formally extended to sediment mixtures consisting of several size-classes represented by diameter d_n for the n'th size-class.

For mixtures the current velocity profiles are obtained with the mean sediment diameter, d_{50}, used to represent the sediment mixture in the evaluation of the movable bed roughness, k_N, and the skinfriction bottom shear stress. The reference concentration is obtained from (26) for the individual size-class with c_b and τ_{cr} replaced by the values corresponding to the particular size-class, d_n. Finally, the concentration of each size class is obtained from (27) through (29) with w_f replaced by w_{fn} and the total mean concentration of suspended sediment is obtained by summation of the contributions from the individual size classes.

It is emphasized that the extension of the model to sediment mixtures, as presented above, is purely formal and based on a number of essentially unsubstantiated generalizations as well as several omissions. Thus, the generalization of the reference concentration formulation to mixtures, which follows the suggestion of Wiberg et al. (1994) is unsubstantiated. In fact, Wilcock and Southard (1988) present data on the initiation of motion of individual size-classes in a mixture that suggest the critical shear stress to be the same for all size-classes, in direct conflict with the proposed generalization. The formal extension of the model to sediment mixtures omits any consideration of armouring effects which ought to be included in a physically realistic manner to produce a complete model. At present the weaknesses of the proposed extension to sediment mixtures become part of the model and are reflected in the empirical determination of model parameters such as the resuspension parameter γ_0, obtained from this model.

Model Application

The hydrodynamic and suspended sediment transport model presented in the preceeding sections contains two parameters that are model-specific: the movable bed roughness, k_N, and the resuspension parameter, γ_0. Thesc parameters and the wind-drag coefficient C_a were determined for an extreme storm event, the "Halloween Storm" of 1991, from a selected subset of field data obtained at the U.S. Army Corps' Field Research Facility (FRF) in 13 m water depth off Duck, North Carolina. For details of field experiments and the data analysis, which produced values of $k_N = 0.144$ cm $\simeq 15\ d_{50}$, $\gamma_0 = 4.0 \cdot 10^{-4}$ and $C_a = 5.0 \cdot 10^{-3}$, the reader is referred to Madsen et al. (1993). Here it suffices to point out that a subset of five bursts of twenty three available were used to obtain the hydrodynamic parameters, k_N and C_a, whereas γ_0 was obtained from analysis of three bursts of twelve available.

Adopting these parameters for the entire storm period, October 27 through November 1, 1991, with wind records from the FRF and augmenting our wave information by use of data from FRF's 8 m pressure sensor array (our tripod surcame to the elements around 18:00 h (EST) on October 30, 1991, when the significant wave height reached $H_s \simeq 4.5$ m with a peak period of $T_p \simeq 20$ s) the required input for application of the model is available.

Figure 1 shows a comparison of predicted and measured longshore (southerly directed when positive) and crosshore (offshore directed when positive) currents at 29 cm above the bottom. The predicted relatively rapid increase in longshore current around 35 h, associated with a rapid increase in wind speed from about 7 m/s to about 16 m/s, preceeds and exceeds the measured currents. The reason for this is most likely the neglect of unsteady effects in the hydrodynamic model formulation. Overall agreement between predicted and observed longshore currents is, however, considered acceptable and quite encouraging given the simplicity of the model. The agreement between predicted and observed crosshore currents is far less striking. Given, however, the very low crosshore currrent velocities the measurements are expected to be extremely sensitive to experimental errors, making detailed point-by-point comparison less meaningful.

Figure 2 shows a comparison of predicted and observed suspended sediment concentrations at 27 cm and 87 cm above the bottom. Considering the fact that only two of the twelve experimental observations at these elevations were used to determine γ_0 the overall agreement between predicted and observed suspended sediment concentrations is very encouraging.

The model results presented in Figures 1 and 2 were obtained without inclusion of a longshore pressure gradient, *i.e.* taking $\partial p/\partial x = 0$. It is of practical interest to point out that the first model run, which was based on the initial estimate of z_{oa} obtained in the manner proposed above, yielded results that were practically indistinguishable from the results obtained after two and three iterations. Also, model runs were performed in which the longshore pressure gradient was estimated from tide records at Virginia Beach and Kitty Hawk, North Carolina, following the procedure described in Chisholm (1993). The inclusion of longshore tidal forcing resulted in only minor modifications of the longshore current of at most 5 cm/s and a negligible (less than 0.2 cm/s) effect on the crosshore velocity. This apparent success of the sediment transport model in its simplest form is, of course, a

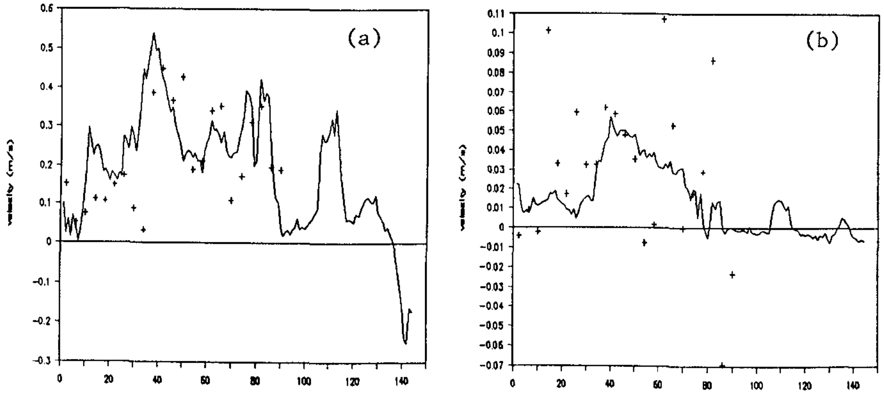

Figure 1: Comparison of measured (crosses) and predicted (full lines) longshore, (a), and crosshore, (b), velocities (m/s) 29 cm above the bottom as a function of time in hours from 0:00 on 27 October, 1991. Measurements at $t = 58, 62, 66, 78$ and 82 hours used in model calibration to obtain k_N and C_a.

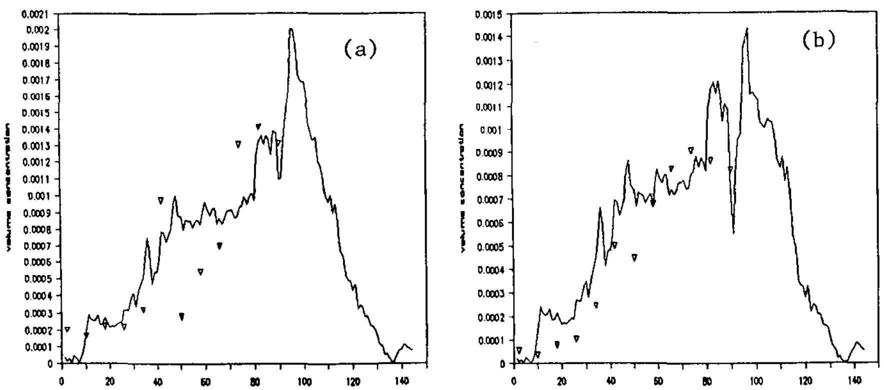

Figure 2: Comparison of measured (triangles) and predicted (full lines) mean suspended sediment concentration (volumetric) at 27 cm, (a), and 87 cm, (b), above the bottom as a function of time in hours from 0:00 on 27 October, 1991. Measurements at $t = 58$ and 66 hours used in model calibration to obtain γ_0.

result of the specific nature of the extreme conditions encountered during the "Halloween Storm" and should not be interpreted to mean that longshore pressure gradients generally may be neglected.

Conclusions

A relatively simple hydrodynamic model for currents induced in inner shelf waters extending from the surf zone to depths of 10 to 20 m along relatively straight coastlines was presented. The model includes Coriolis effect and wave-current interactions in the bottom boundary layer and predicts the current velocity profiles in both the longshore and crosshore directions.

The hydrodynamic model is coupled with a model for the prediction of the mean suspended sediment concentration to produce a mean suspended sediment transport model for inner shelf coastal waters.

The capabilities of the model were illustrated by its application to an extreme storm event, the "Halloween Storm", for which field data were available for comparison with model predictions. The limited comparison presented in this paper will be expanded upon in forthcoming publications. However, the comparison between predictions and observations presented here suggests an accuracy of within a factor of two to be achievable when the model is properly calibrated. This conclusion is further supported by computations of the net loss of sediment volume per meter of beach during the entire Halloween Storm. The model's predictions of a loss of about 22 m^3 per meter compares favorably with losses of 27 and 54 m^3 per meter beach obtained from profile surveys from before and after the "Halloween Storm" by the FRF along transects north of the FRF pier.

It is believed that the model presented here may serve the role of providing the important link between surf zone sediment transport processes and those in deeper waters of the continental shelf.

Acknowledgements This study was supported by the National Science Foundation, Marine Geology and Geophysics Grant OCE-9017828. Bill Birkemeier, Kent Hathaway, Chuck Long, and their colleagues at the U.S. Army Corps Field Research Facility (FRF) at Duck, NC, are thanked for retrieving the remains of our tripod, for providing the wave and wind data recorded by the FRF, and for their ongoing cooperation.

References

Abramowitz, M., I.A. Stegun (1972) *Handbook of Mathematical Functions*, National Bureau of Standards Applied Math Series, No. 55, pp. 379-509.

Chisholm, T.A. (1993) Analysis of field data on near-bottom turbulent flows and suspended sediment concentrations, Eng. Thesis, Dept. Civil & Environmental Engineering, MIT.

Jenter, H.L., O.S. Madsen (1989) Bottom stress in wind-driven depth-averaged coastal flows. *Journal Physical Oceanography* 19(7):962-974.

Madsen, O.S. (1977) A realistic model of the wind-induced Ekman boundary layer. *Journal Physical Oceanography* 7(2):248-255.

Madsen, O.S. (1991) Mechanics of cohesionless sediment transport in coastal waters. *Proceedings Coastal Sediments '91*, ASCE, Seattle. 1:15-27.

Madsen, O.S. (1994) Spectral wave-current bottom boundary layer flows. *Proceedings 24th ICCE*, ASCE, Kobe, Japan.

Madsen, O.S., W.D. Grant (1976) Quantitative description of sediment transport by waves. *Proceedings 15th ICCE*, ASCE, Honolulu. 2:1093-1112.

Madsen, O.S., D.L. Wright, J.D. Boon, T.A. Chisholm (1993) Wind stress, bed roughness, and sediment suspension on the inner shelf during an extreme storm event. *Continental Shelf Research* 13(11):1303-1324.

Smith, J.D., S.R. McLean (1977) Spatially averaged flow over a wavy surface. *Journal Geophysical Research* 82:1735-1746.

Wiberg, P.L., C.K. Harris (1994) Ripple geometry in wave-dominated environments. *Journal Geophysical Research* 99(C1):775-790.

Wiberg, P.L., D.E. Drake, D.A. Cacchione (1994) Sediment resuspension and bed armoring during high bottom stress events. *Continental Shelf Research* 14(10/11):1191-1220.

Wikramanayake, P.N. (1992) Velocity profiles and suspended sediment transport for combined turbulent wave-current flows. Ph.D. Thesis, Dept. Civil & Environmental Engineering, MIT.

Wilcock, P.R., J.B. Southard (1988) Experimental study of incipient motion in mixed-size sediments. *Journal Water Resources Research* 24(7):1137-1151.

Wu, J.J. (1982) Wind-stress coefficients over sea surface from breeze to hurricane. *Journal Geophysical Research* 87:9704-9706.

Appendix A: Approximate Determination of $\partial p/\partial x$

If evidence of pronounced variations in mean water level along the coastal section under consideration is available, *e.g.* from tide gauge records, it may not be safe to assume the alongshore pressure gradient to be zero. To estimate the effect of a nonzero longshore pressure gradient it is assumed that an estimate of the mean surface slope, as a function of time, is available for the location of interest, *i.e.* the pressure gradient driving a longshore flow is given by $\rho g \partial\bar{\eta}/\partial x$. In the absence of any Coriolos forcing in the x-direction ($V = 0$) the equation governing the depth-averaged longshore velocity U induced by the pressure gradient in water depth h is

$$\frac{\partial U}{\partial t} = -g\frac{\partial \bar{\eta}}{\partial x} - (C_b/h)|\bar{u}|U \tag{A.1}$$

in which $|\bar{u}|$ is the depth-averaged longshore velocity obtained from the depth-resolving model solution, *i.e.*

$$|\bar{u}| = \frac{1}{h}\int_0^h \Re\{W_{Ug}\}dz \tag{A.2}$$

with W given by (8) and (9). Since model application is limited to water depths of 10 to 20 m or less, it is reasonable to assume that the longhsore velocity is closely described by the logarithmic profile up to half-depth, *i.e.* up to $z = h/2$, and that the velocity at $z = h/2$ is a close approximation to the depth-averaged total longshore velocity (wind-induced as well as pressure gradient driven). It follows from these considerations that the bottom drag coefficient, C_b, is related to the apparent bottom roughness z_{oa}, which is known from (16) of the depth-resolving model, through

$$\sqrt{C_b} = \frac{\kappa}{\ell n \frac{h}{2z_{oa}}} \tag{A.3}$$

With $|\bar{u}|$ and C_b known as functions of time from the depth-resolving model, (A.1) may be solved numerically for the given temporal variation of $\partial\bar{\eta}/\partial x$.

The solution for U obtained in this manner includes unsteady effects which were considered negligible in the depth-resolving model formulation. However, the exact same time-varying longshore velocity U could have been obtained from a steady form of (A.1) if the pressure gradient term, $\frac{\partial \bar{\eta}}{\partial x}$ in (A.1) were replaced by an equivalent steady pressure gradient

$$-\frac{1}{\rho}\frac{\partial p}{\partial x} = \frac{C_b}{h}|\bar{u}|U \tag{A.4}$$

Thus solving (A.1) for U and subsequent evaluation of (A.4) will produce a longshore pressure gradient which, when introduced in the steady depth-resolving model, will return practically the same estimate of the longshore pressure gradient driven velocity as obtained from (A.1). If the addition of the longshore pressure gradient determined from (A.4) leads to drastic modifications of the depth-resolving model's predictions of $|\bar{u}|$ and C_b it may be necessary to use this procedure in an iterative manner until convergence has been achieved.